Radiation Response of a MEMS Accelerometer: An Electrostatic Force*

L.D. Edmonds, C.I. Lee, and G.M. Swift
Jet Propulsion Laboratory
California Institute of Technology
Pasadena, CA

Abstract

Particle irradiation on the mechanical sensor of the ADXL50 microelectromechanical accelerometer shifts the output voltage. An earlier conclusion, that a dielectric below the sensor becomes charged, is extended by quantifying the effect of this charge on device output. It is shown that an electrostatic force is consistent with the observation that the output voltage shift is independent of acceleration. An appendix derives a convenient algorithm for calculating electrostatic forces, which may also be used for other MEMS devices.

I. INTRODUCTION

The Analog Devices ADXL50 accelerometer is a microelectromechanical system (MEMS) containing a mechanical structure (sensor), part of which moves under acceleration, and electronics integrated on the same chip. The output voltage is a measure of the acceleration. Earlier work [1,2] indicated that ionization effects in both the sensor and electronics contributed to the radiation response of the device. Restricting the irradiation, via an aperture, to hit only the sensor caused a shift in the output voltage. Knudson *et al.* [1] have demonstrated that the output voltage shift is caused by the charging of a dielectric below the sensor. The present paper provides a more complete explanation by quantitatively analyzing the effect that dielectric charging should have on device operation.

II. DEVICE OVERVIEW

A high-level discussion of device operation is presented here. Interested readers are referred to Ref.[3] for details. A functional diagram of the ADLX50 is shown in Fig.1. The sensor is symbolically represented by one moveable electrode (ME) between two fixed electrodes. The three electrodes form two capacitors in series, shown as C_1 and C_2 in the figure. Voltages with a "~" superscript are AC and all others are DC.

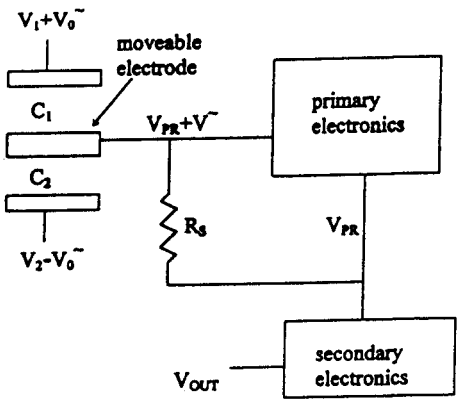

Fig.1: Functional Diagram of the Device.

The voltages V_1, V_2, and V_0^- are fixed. A force applied to the ME (usually a pseudo-force produced by accelerating the device) tends to displace it from the center position. This force is balanced partly by a mechanical spring constant (not shown in the figure), but primarily by electrostatic forces produced by V_1, V_2, and V_{pr} (more will be said about this later). The end result is that the applied force produces some displacement of the ME. This displacement changes C_1 and C_2, which changes V^- shown in the figure. This voltage is the input to the primary circuit. The response to this AC input is a DC output voltage V_{pr}, which is the most direct DC measure of the ME position. During closed loop operation (the case represented in the figure), this DC voltage is transmitted to the ME. Resistor R_S isolates AC from DC voltages in the sense that it simulates a short for DC voltages and an open circuit for AC voltages. To the extent that the primary circuit can be approximated as ideal, its input current is zero (both AC and DC). Therefore the AC voltage at the ME is completely determined by the ME position, while the DC voltage at the same location is completely determined by the primary circuit output. The primary circuit is designed so that V_{pr} responds to V^- in such a way that the electrostatic forces produced by the DC voltages in the sensor oppose the applied force. The result is that the ME displacement is much smaller than it would be if the applied force was balanced by the mechanical spring constant alone. Limiting the displacement to small values improves device linearity. The voltage V_{pr} has a fixed calibration and

* The work described in this paper was carried out by the Jet Propulsion Laboratory, California Institute of Technology, under contract with the National Aeronautics and Space Administration Code S. Work funded by the NASA Microelectronics Space Radiation Effects Program (MSREP).

can only be monitored by high-impedance instrumentation. The secondary circuit converts V_{pr} into a more conveniently calibrated V_{out} (the user has some control over this calibration) which can be monitored by lower impedance instrumentation.

A more literal representation of the sensor, illustrated in Fig.2, shows that C_1 and C_2 are each parallel combinations of many capacitors which can be grouped into unit cells. Fig.2 shows four unit cells, but the entire sensor contains 42 such cells. The ME voltage is represented as V_3 in this figure to include the most general possible conditions (Fig.1 refers to closed-loop operation, but there is also a self-test mode in which $V_3 \neq V_{pr}$). This top view does not show the dielectric, which is crucial to this investigation. The dielectric is below the electrodes [1], as illustrated in Fig.3 (the charges and electric field lines are discussed later). Below the dielectric is a conducting medium (a silicon substrate) held at the same potential as the ME to inhibit vertical electrostatic forces on the ME [1]. The intended motion of the ME is horizontal in Fig.3.

III. THE PROPOSED EXPLANATION

Knudson *et al.* [1] have experimentally demonstrated that dielectric charging is responsible for the output voltage shift observed after sensor irradiation. However, their work did not explain *why* dielectric charging should shift the output voltage. Note that dielectric charging will not influence the AC voltages (and hence cannot influence V_{out}), except indirectly by moving the ME via an electrostatic force. This strongly suggests that an electrostatic force is involved, but leads to a question. It is easy to see how a force produced by the dielectric charge might move the ME vertically, but this does not explain the observed data. If the ME is horizontally centered, there should be a null reading at the device output even if there is a vertical displacement, i.e., a vertical displacement might change the device sensitivity, but is not expected to produce an offset in the device output. However, data reported by Lee *et al.* [2] show the opposite effect. When the output voltage is plotted against acceleration, the effect of electrostatic charging is seen as a vertical translation (or offset) of this plot, with no change in slope (or sensitivity). The vertical translation of the plot indicates that a constant horizontal force is added to the applied force on the ME. The question is how the charged dielectric can exert a horizontal force on the ME.

The explanation is illustrated in Fig.3. Nominal charges and electric fields are defined here to be those produced by the electrode biasing voltages in the absence of a dielectric charge. A horizontal electric field line in Fig.3 represents a nominal field line connecting a nominal positive charge on one electrode to a nominal negative charge on another. If the ME is centered, its biasing voltage is adjusted (via the primary circuit) so that the force, produced by the nominal fields acting on the nominal charges, on one side of the ME is balanced by the force on the other side. A dielectric charge upsets this balance by creating induced image charges in the ME. A fringing electric field line in Fig.3 begins on a fixed positive

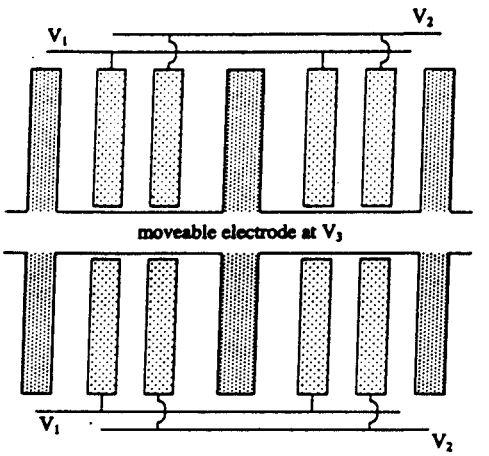

Fig.2: Top view (not to scale) of four cells in the sensor.

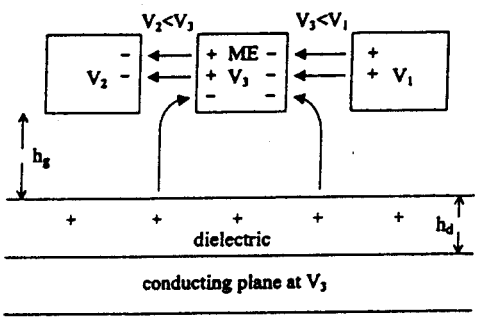

Fig.3: Side view of one sensor cell illustrating the horizontal force. For a positively charged dielectric, the resulting field (nominal plus fringing) and net charge (nominal plus induced) are both stronger on the right side of the ME.

(in this illustration) charge in the dielectric and ends on a negative induced charge in the ME. The fringing and nominal fields add on the right side of the ME, but subtract on the left, so the resulting field is stronger on the right. The nominal and induced charges have the same polarities on the right side of the ME, but opposite polarities on the left, so the net charge is greater (in absolute value) on the right. The stronger electric field acting on the stronger charge on the right side of the ME pulls the ME to the right.

A quantitative analysis of this force is derived in the appendix. The analysis concludes that the horizontal force on the ME can be expressed as a sum of two terms. The first term is the nominal force that would be present under the same biasing conditions but with an uncharged dielectric. The second term is proportional to the dielectric charge and is the excess force that is of interest here. This excess force depends on V_1-V_2 and on physical parameters describing the sensor and dielectric, but does not depend on the ME position or on V_3. This is significant because when plotting device output versus acceleration, the ME position and V_3 both vary, but V_1 and V_2 are fixed. Therefore the excess force is a constant, so its influence should be seen as a vertical translation of the plot, consistent with data presented by Lee *et al.* [2].

The excess force, denoted here as f, is the force per unit cell calculated by (A32) in the appendix, multiplied by 42 cells. The result is

$$\frac{f}{M}=\frac{21}{M}\frac{Lh_{eff}\,\sigma}{h_g\frac{\varepsilon_{eff}}{\varepsilon_0}+h_d}(V_1-V_2)$$

where M is the ME mass and the other symbols are explained below. The left side is written as f/M, which is the acceleration needed to produce a pseudo-force equal to f, because device calibration data refer to acceleration. The dimensions h_g and h_d are shown in Fig.3, and L is electrode length (into the page in Fig.3). The ratio $\varepsilon_{eff}/\varepsilon_0$ is the relative dielectric constant for a homogeneous dielectric, or an effective relative dielectric constant for an inhomogeneous dielectric. The quantity σ is the dielectric charge per unit area. The quantity h_{eff} is a weighted-average, or effective, height (above the lower electrode) of the charge distribution in the dielectric. If the dielectric is homogeneous and the charge is confined to a narrow layer, h_{eff} is the height of this layer. If the dielectric is inhomogeneous, h_{eff} may not be the actual height. However, whether or not the dielectric is homogeneous, $h_{eff}\approx h_d$ if the dielectric charge is close to the upper dielectric surface. Note that the force decreases if h_{eff} decreases with σ held fixed. This is because charges closer to the lower electrode induce greater image charge in this electrode and less image charge in the upper electrodes.

For numerical evaluation, note that the dielectric consists of a 60 nm layer of Si_3N_4 above a 120 nm layer of SiO_2 [1]. The relative dielectric constants of the upper and lower materials are 7.5 and 3.9, respectively. Calculating ε_{eff} from equation (A20) in the appendix gives $\varepsilon_{eff}/\varepsilon_0=4.64$. We also have $h_d=180$ nm [1], $h_g=1.6$ μm [1], M=0.16 μg [4], L=120 μm [4], and $V_1-V_2=3.2$ volts [3]. Substituting these numbers into the above equation gives

$$\frac{f}{M}=K_1\frac{h_{eff}}{h_d}\sigma,\quad K_1=1.95x10^{-10}g\left(\frac{q}{cm^2}\right)^{-1}\quad(1)$$

which conveniently calculates f/M in units of the gravitational acceleration g if $(h_{eff}/h_d)\sigma$ is expressed in units of elementary charge per cm^2. The sign convention is such that f is positive when it moves the ME up in Fig.1 (or to the right in Fig.3). The primary circuit is designed so that a displacement in this direction increases V_{pr}. This voltage is inverted in the secondary circuit, so V_{out} decreases. Therefore, a positive σ should decrease V_{out}, and a negative σ should increase V_{out}.

IV. CHARGING MECHANISMS

Lee *et al.* [2] investigated the effects from both protons and electrons when used for sensor-only irradiation. The electrons were supplied by a scanning electron microscope (SEM). Although difficult to analytically quantify, charging under SEM irradiation is familiar. Charging of a dielectric (e.g., a passivation layer) is a contest between the emission of low-energy secondary electrons, and the absorption of higher-energy electrons backscattered from other locations (e.g., a substrate below a passivation layer) [5]. The relative importance of the latter mechanism to the former is greatest when the primary electrons are high-energy and hit the device at normal incidence [5]. It is empirically known that dielectrics typically charge negative when the primary electrons hit the device at normal incidence at energies greater than 10 KeV [5]. Lee *et al.* [2] used 30 KeV electrons (most of which will still have energies exceeding 10 KeV after penetrating the 2 μm thick electrodes before reaching the dielectric) at normal incidence, so we expect a negatively charged dielectric. This irradiation was found to increase V_{out}, consistent with the earlier prediction that a negatively charged dielectric should increase V_{out}.

Knudson *et al.* [1] and Lee *et al.* [2] both found V_{out} to decrease following sensor-only irradiation by protons, indicating a positively charged dielectric. If the charging mechanisms are the same as for SEM irradiation, we conclude that secondary electron emission dominates backscattered electron absorption for the proton case (other charging mechanisms might also be considered as discussed later). Some of the data presented by Knudson *et al.* [1] are reproduced in Fig.4, showing V_{out} as a function of 0.96 MeV proton fluence. The figure shows that V_{out} saturates, indicating that some other mechanism competes with the charging mechanism and limits the accumulated charge. The most obvious competing mechanism is a charge-induced attractive force that pulls secondary electrons back to the dielectric. However, it will be argued later that this does not explain the data, and there must be another competing mechanism that becomes important even before charging is sufficient to significantly impede secondary electron escape. A possible competing mechanism is a proton-induced generation of mobile electron-hole pairs in the dielectric which move in response to the electric field. Knudson *et al.* [1] suggested that carriers generated by the protons are ultimately responsible for dielectric charging. We suggest the opposite, that this mechanism is a response that limits accumulated charge. However, our suggestion that charging is by secondary

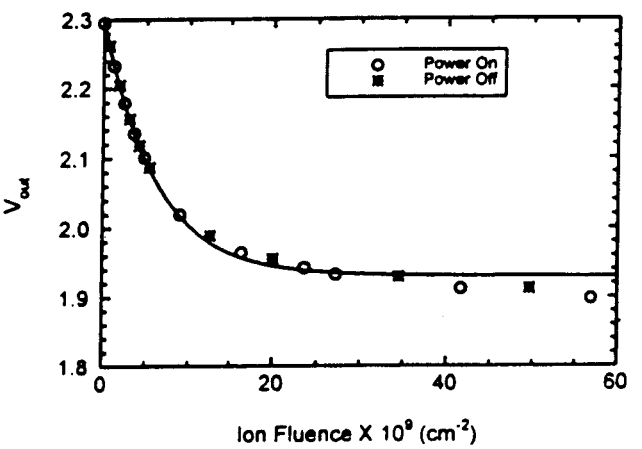

Fig.4: V_{out} as a function of proton fluence from Knudson *et al.* [1]. The smooth curve, originally reported as an empirical fit, is predicted by (3) with suitably chosen α and β.

electrons may have trouble explaining some of the data. The Knudson *et al.* data reproduced in Fig.4 include two cases; the device is biased (V_1=3.4 volts, V_2=0.2 volts, and V_3=1.8 volts) and unbiased during irradiation. There is almost no difference between the two cases. We have not quantitatively analyzed this, but it seems reasonable to expect the two cases to differ if secondary electron emission really is the charging mechanism. Additional research is needed.

Whatever the charging and competing mechanisms are, charging and discharging rates under the conditions represented by Fig.4 can be quantified with help from (1). Let $\Delta\sigma$ be the net increase in σ produced by an increment ΔF of proton fluence. Then $\Delta\sigma=\Delta_1\sigma-\Delta_2\sigma$ where $\Delta_1\sigma$ is the increase produced by the charging mechanism, and $\Delta_2\sigma$ is the decrease produced by the competing mechanism. We assume that the first term is proportional to the fluence, i.e., $\Delta_1\sigma=q\alpha(h_d/h_{eff})\Delta F$ for some constant α. The factor h_d/h_{eff} is included for later convenience. If charging is by secondary electrons, the charge will be near the top of the dielectric, so $h_d/h_{eff}\approx 1$, and α is the secondary electron yield (average number of electrons emitted for each proton hit). For any other charging mechanism, α is an effective yield. The loss term is assumed to be proportional to both ΔF and σ, i.e., $\Delta_2\sigma=\beta\sigma\Delta F$ for some constant β. The resulting equation becomes $d\sigma/dF=q\alpha(h_d/h_{eff})-\beta\sigma$ with solution

$$\frac{h_{eff}}{h_d}\sigma = q\frac{\alpha}{\beta}\left[1-\exp(-\beta F)\right]. \qquad (2)$$

Substituting for σ in (1) and using calibration data reported by Knudson *et al.* [1] to convert f/M into V_{out} gives

$$V_{out} = V_0 - K_2\frac{\alpha}{\beta}\left[1-\exp(-\beta F)\right] \qquad (3)$$

where V_0=2.3 volts and $K_2=8.78\times10^{-9}$ mV-cm^2. The smooth curve in Fig.4 was originally reported as an empirical fit, but the same curve is produced by (3) if α=6.9 and $\beta=1.64\times10^{-10}$ cm^2. Credibility of secondary electron emission as the charging mechanism can be tested by considering the number 6.9 calculated for α. If this is the mechanism, the secondary electron yield should be 6.9. The actual yield is not known, but 6.9 is the expected order of magnitude. The yield for 1 MeV protons on Al is about 1.0 [6], and the yield is slightly larger for protons that are slowed down by the electrodes before reaching the dielectric. The yield for Si_3N_4 is probably several times that for Al, possibly more if Si_3N_4 behaves like a cathode. Therefore, secondary electron emission presently appears to have some credibility.

It was previously promised that an argument would be given indicating that an attractive force pulling secondary electrons back to the dielectric is too weak to be the competing mechanism limiting the charge. The argument notes that the potential barrier that secondary electrons must escape, when irradiation is without biasing voltages, is the potential of the upper dielectric surface relative to the upper grounded electrodes (which is also the potential across the dielectric). This is calculated from (A23) in the appendix. The limiting value of $(h_{eff}/h_d)\sigma$ is seen from (2) to be $q\alpha/\beta$, which is calculated from the numbers given above to be 4.2×10^{10}q/cm^2. Using the dielectric parameters previously listed, the potential barrier produced by this limiting value of $(h_{eff}/h_d)\sigma$ is calculated to be 0.29 volts. This applies when the charge is at its limiting value, i.e., when competing mechanisms prevent any further charging. In view of the fact that a typical secondary electron energy is about 2 eV [6], it seems unlikely that this potential barrier will completely stop any further charging. However, 0.29 volts across a 0.18 μm thick dielectric creates a strong electric field there, so a current through the dielectric (containing proton-induced mobile carriers) may be a credible competing mechanism.

V. CONCLUSIONS

The response of the ADXL50 to irradiation when the sensor (alone) is irradiated is believed to be the result of electrostatic forces produced by dielectric charging. The charging mechanism induced by SEM irradiation is familiar, though difficult to analytically quantify. The charging mechanism induced by proton irradiation is less certain. The charging rate under Fig.4 conditions has the order of magnitude expected from secondary electron emission in the absence of biasing voltages, but this mechanism may not be consistent with the observation that biasing voltages have almost no effect on the charging rate. Additional research is needed. However, it is clear that electron and proton irradiation can shift the output voltage in opposite directions, so one environment is not equivalent to another having the same total ionizing dose (TID) measure.

The notable difference between electron- and proton-induced responses indicates that the relevant charging mechanisms differ from those most familiar from TID investigations of other devices. A suggested explanation is as follows. While TID can lead to dielectric charging, creating an electric field that can adversely affect the performance of some devices, the relevant electric field is typically inside the device. For conventional devices, an electric field outside the device is not relevant, and may not even be present. If the electric field outside the device produced by the dielectric charge is not already nullified by image charges in nearby conductive structures, we would expect ambient charged particles to accumulate on exposed dielectric surfaces until there is no longer an external field. If the charge on an exposed dielectric is very close to the surface (as expected for secondary electron emission), ambient charges that nullify the electric field outside the dielectric do so by completely compensating for the dielectric charge, so that there is no net surface charge. Therefore, we would not expect secondary electron emission to be an important radiation concern for the performance of conventional devices.

In contrast, the electric field creating a force on the MEMS ME is above an exposed dielectric. Note that, regardless of what the charging mechanism is, it is reasonable to expect ambient charged particles accumulating on the dielectric surface to weaken this force. However, Knudson *et al.*[1]

report very little recovery from a two day anneal at 150°C following sensor-only irradiation by protons. A suggested explanation is that very few ambient charged particles are able to get past the upper electrodes to reach the dielectric. The result is that the electric field above the dielectric created by the dielectric charge is not nullified. Therefore, a charging mechanism such as secondary electron emission may be important for this MEMS, even though it may not affect the performance of more conventional devices.

Whether or not the explanations suggested above are correct, it is still true that TID is not an adequate measure of the environment for this MEMS, because electrons produce a different response than protons. Similar effects might be seen in other MEMS structures, which mandates testing in both electron and proton environments.

REFERENCES

[1] A.R. Knudson, S. Buchner, P. McDonald, W.J. Stapor, A.B. Campbell, K.S. Grabowski, D.L. Knies, S. Lewis, and Y. Zhao, "The Effects of Radiation on MEMS Accelerometers," *IEEE Trans. Nucl. Sci.*, vol.43, pp.3122-3126, Dec. 1996.

[2] C.I. Lee, A.H. Johnston, W.C. Tang, C.E. Barnes, and J. Lyke, "Total Dose Effects on Microelectromechanical Systems (MEMS): Accelerometers," *IEEE Trans. Nucl. Sci.*, vol.43, pp.3127-3132, Dec. 1996.

[3] Analog Devices Data Book, "Monolithic Accelerometer with Signal Conditioning: ADXL50."

[4] W. Kuehnel, "Modelling of the Mechanical Behaviour of a Differential Capacitor Acceleration Sensor," *Sensors and Actuators*, A 48, pp.101-108, 1995.

[5] J.R. Devaney, K.O. Leedy, and W.J. Keery, *Notes on SEM Examination of Microelectronic Devices*, NBS special publication 400-35, April 1977.

[6] H.B. Garrett and C.P. Pike (editors), *Space Systems and Their Interactions with Earth's Space Environment*, New York University New York, p.173, 1980.

APPENDIX: CALCULATION OF FORCE

Electrostatic forces exerted on a charged conductor can be calculated by calculating the energy stored in the electrostatic field as a function of the location of the conductor, and then noting how the stored energy changes when the conductor is moved. The basic idea is familiar, but convenient computational algorithms are not easily found in the literature. One such algorithm, utilizing "elementary potentials", is derived here for the general case, and then applied to the specific case considered in the main text.

A1. *The Physical Arrangement*

The analysis applies to an arbitrary collection of conductors and dielectric structures contained within a region of space denoted R. These conductors form at least part of the boundary surface of R, but the theory requires R to have a closed boundary surface. The boundary surface can consist of any combination of conducting surfaces and/or reflective surfaces. A reflective surface is defined by the property that the normal component of the electric field is zero. An example of such a region is shown in Fig.A1. Surfaces S_1, S_2, etc. are conductors, and surfaces represented by dashed lines are reflective. If R extends to infinity, it can be closed by imagining a conducting surface at infinity, which is also denoted by an S with a subscript, so that the closed boundary of R consists of the surfaces S_1, S_2, etc., together with the reflective boundaries (if any).

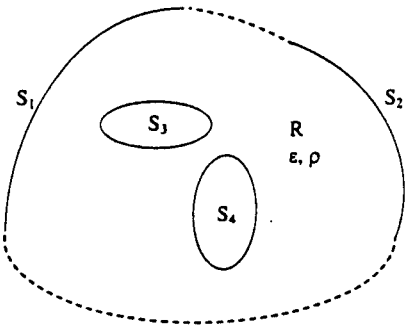

Fig.A1: An example of a region R having a closed boundary consisting of conductive surfaces (solid lines) and/or reflective surfaces (dashed lines). Dielectric structures are included by allowing ε and ρ to be functions of position.

Dielectric materials contained within R are required to be isotropic, but need not be homogeneous. If any dielectric materials are in direct contact with the conductor at which the force is to be calculated, there may be mechanical forces between the dielectric and conductor, which are not calculated in the analysis to follow. Dielectric structures are not shown in Fig.A1, because such structures are represented by allowing the dielectric constant ε to be a function of the spatial coordinates within R. Immobile free charge embedded in the dielectric is described by a volume charge density ρ, which is a function of the spatial coordinates within R. It is mathematically convenient to assume that both ε and ρ are well-behaved functions of the spatial coordinates within R. Discontinuities in ε and/or surface charges on the boundaries of dielectric structures can be treated by taking limits.

The objective is to calculate the electrostatic force on any selected conductor within R, which will be called the "selected conductor".

A2. *Elementary Potentials*

Let N be the number of conducting surfaces which, when combined with reflective surfaces (if any), form a closed boundary for R. The elementary potentials ϕ_0, ϕ_1, ...,ϕ_N are defined for future use by

$$\vec{\nabla} \circ [\varepsilon \vec{\nabla} \phi_0] = -\rho \quad in\ R \qquad (A1a)$$

$$\phi_0 = 0 \quad on\ S_i\ (i = 1,...,N) \qquad (A1b)$$

$$\vec{\nabla} \circ [\varepsilon\, \vec{\nabla}\phi_i] = 0 \quad in\ R\ (i = 1,...,N) \qquad (A2a)$$

$$\phi_i = 1\ on\ S_i, \quad \phi_i = 0\ on\ S_j\ if\ j \neq i \quad (i, j = 1,...,N) \qquad (A2b)$$

with reflective boundary conditions tacitly assumed on the reflective boundaries. The elementary potentials are not all independent. The sum in i of ϕ_i for i=1,...,N satisfies the homogeneous equation (A2a), reflective boundary conditions on the reflective boundaries, and equals 1 on all other boundary sections. The solution to this boundary value problem is 1, so

$$\sum_{i=1}^{N} \phi_i = 1. \qquad (A3)$$

Equations to follow are conveniently written in terms of a $C_{i,j}$ array defined by

$$C_{0,0} \equiv \int_R \varepsilon\, \vec{\nabla}\phi_0 \circ \vec{\nabla}\phi_0\, d^3x \qquad (A4a)$$

$$C_{0,j} \equiv -\int_R \phi_j\, \rho\, d^3x \quad (j = 1,...,N) \qquad (A4b)$$

$$C_{i,j} \equiv \int_R \varepsilon\, \vec{\nabla}\phi_i \circ \vec{\nabla}\phi_j\, d^3x \quad (i, j = 1,...,N). \qquad (A4c)$$

Future steps will explicitly calculate the C's, and the defining equations are not necessarily the most convenient for this purpose. Alternate expressions can be obtained via the divergence theorem. For example, if we first use (A1b), then the divergence theorem, and then (A1a), we obtain

$$0 = \oint \phi_0\, [\varepsilon\, \vec{\nabla}\phi_0] \circ d\vec{S} =$$

$$\int_R \vec{\nabla}\phi_0 \circ [\varepsilon\, \vec{\nabla}\phi_0]\, d^3x + \int_R \phi_0\, \vec{\nabla} \circ [\varepsilon\, \vec{\nabla}\phi_0]\, d^3x =$$

$$\int_R \varepsilon\, \vec{\nabla}\phi_0 \circ \vec{\nabla}\phi_0\, d^3x - \int_R \phi_0\, \rho\, d^3x$$

so that

$$C_{0,0} = \int_R \phi_0\, \rho\, d^3x. \qquad (A5a)$$

Similar steps give

$$\int_{Si} \varepsilon\, \vec{\nabla}\phi_0 \circ d\vec{S} =$$

$$\oint \phi_i\, [\varepsilon\, \vec{\nabla}\phi_0] \circ d\vec{S} - \oint \phi_0\, [\varepsilon\, \vec{\nabla}\phi_i] \circ d\vec{S} =$$

$$\int_R \vec{\nabla}\phi_i \circ [\varepsilon\, \vec{\nabla}\phi_0]\, d^3x + \int_R \phi_i\, \vec{\nabla} \circ [\varepsilon\, \vec{\nabla}\phi_0]\, d^3x$$

$$- \int_R \vec{\nabla}\phi_0 \circ [\varepsilon\, \vec{\nabla}\phi_i]\, d^3x - \int_R \phi_0\, \vec{\nabla} \circ [\varepsilon\, \vec{\nabla}\phi_i]\, d^3x =$$

$$- \int_R \phi_i\, \rho\, d^3x$$

where the unit normal vector in all surface integrals is outward from the interior of R (into the conductors). Combining the above result with (A4b) gives

$$C_{0,j} = \int_{Sj} \varepsilon\, \vec{\nabla}\phi_0 \circ d\vec{S} \quad (j = 1,...,N). \qquad (A5b)$$

Similar steps give

$$C_{i,j} = \int_{Si} \varepsilon\, \vec{\nabla}\phi_j \circ d\vec{S} =$$

$$\int_{Sj} \varepsilon\, \vec{\nabla}\phi_i \circ d\vec{S} \quad (i, j = 1,...,N). \qquad (A5c)$$

Note that the C's are not all independent. For example, it is obvious from the above equations that

$$C_{i,j} = C_{j,i}. \qquad (A6a)$$

Two more constraints are obtained by combining (A3) with (A4b) and (A4c) to get

$$\sum_{j=1}^{N} C_{0,j} = -\int_R \rho\, d^3x \qquad (A6b)$$

$$\sum_{j=1}^{N} C_{i,j} = 0 \quad (i = 1,...,N). \qquad (A6c)$$

The signs of some of the C's can be predicted for the general case. It is obvious from (A4c) that

$$C_{ii} \geq 0 \quad (i = 1,...,N). \qquad (A7a)$$

Also, note that ϕ_i=1 on S_i, and ϕ_i=0 on S_j for j≠i, so ϕi decreases as the observation point moves to S_j, i.e., the gradient of ϕ_i is directed away from S_j. The unit normal vector is directed into S_j, so we conclude from (A5c) that

$$C_{i,j} \leq 0 \quad if\ i \neq j \quad (i, j = 1,...,N). \qquad (A7b)$$

A3. *Expressions for Charge and Energy*

Let each conductor S_i be at a potential V_i and carry a charge Q_i. Let ϕ be the potential produced by this arrangement, so ϕ satisfies

$$\vec{\nabla} \circ [\varepsilon\, \vec{\nabla}\phi] = -\rho \quad in\ R$$

$$\phi = V_i \quad on\ S_i \quad (i = 1,...,N)$$

with reflective boundary conditions tacitly assumed on the reflective boundaries. The motivation for defining the elementary potentials is that ϕ can be expressed as

$$\phi = \phi_0 + \sum_{i=1}^{N} V_i\, \phi_i \qquad (A8)$$

which can be verified by using (A1) and (A2) to conclude that the right side satisfies the same boundary value problem as the left side.

The energy U stored in the electrostatic field is given by the well-known equation

$$U = \frac{1}{2} \int_R \varepsilon\, \vec{\nabla}\phi \circ \vec{\nabla}\phi\, d^3x.$$

One motivation for defining the C's is that after substituting (A8) into the above equation and expanding the product of sums, the resulting expression will contain terms appearing on the right sides of (A4a) and (A4c), plus some additional terms that can be shown to be zero from the divergence theorem. Using (A4) to express the non-vanishing terms in terms of the C's gives

$$U = \frac{1}{2} C_{0,0} + \frac{1}{2} \sum_{i,j=1}^{N} C_{i,j}\, V_i\, V_j. \qquad (A9)$$

The Q's can also be expressed in terms of the C's. We start with Gauss's law

$$Q_i = \int_{Si} \varepsilon \vec{\nabla}\phi \circ d\vec{S}$$

and use (A8) to substitute for ϕ, and then use (A5) to obtain

$$Q_i = C_{0,i} + \sum_{j=1}^{N} C_{i,j} V_j \quad (i = 1,...,N). \quad (A10)$$

A4. *Electrostatic Force*

Let $\mathbf{X_C}$ refer to some fixed point on the selected conductor, so that a change in $\mathbf{X_C}$ represents a translation of this conductor. All other conductors and dielectric structures are imagined to be held in fixed positions when the selected conductor is translated. Arbitrarily small translations are sufficient for the analysis to follow, so it is not necessary for the physical system to make sense for all $\mathbf{X_C}$ (e.g., that places the selected conductor inside of another conductor, or outside of R). It is only necessary for the physical system to make sense for $\mathbf{X_C}$ in some arbitrarily small neighborhood of the actual location of the selected conductor. With the selected conductor now imagined to be movable, the C's become functions of $\mathbf{X_C}$. Instead of $C_{i,j}$, we now write $C_{i,j}(\mathbf{X_C})$. Similarly, instead of U, we now write $U(\mathbf{X_C})$.

Suppose an external force is applied to the selected conductor, and is adjusted so that it nearly balances the electrostatic force, allowing the selected conductor to be displaced with a negligible change in kinetic energy. If the selected conductor is displaced, the external force does some work, and there is also a change in the energy of the system. With some qualifications (discussed below), this work equals the change in energy. There is no change in kinetic energy, so the work done by the external force equals the change in U, implying that the external force is the gradient (in the $\mathbf{X_C}$ coordinates) of $U(\mathbf{X_C})$. The electrostatic force balances the external force, so the electrostatic force $\mathbf{F}$ is the negative of this gradient, i.e.,

$$\vec{F} = -\vec{\nabla}_C U(\vec{X}_C) \quad (A11)$$

where the subscript to the gradient operator refers to the $\mathbf{X_C}$ coordinates.

Two qualifications are needed for (A11) to be valid. An early assumption leading to (A11) is that the work done by the external force equals the change in energy of the system. Therefore, one qualification is that there are no other agents exchanging energy with the system. In particular, there can be no voltage sources exchanging charge and energy with the conductors while the selected conductor is displaced. If there are any voltage sources forcing the conductors to be at the potentials $V_1,...,V_N$, these sources must be disconnected during the time that the selected conductor is displaced. Therefore, the Q's, and not the V's, are regarded as constants when $\mathbf{X_C}$ is changed. This requires that the V's change as $\mathbf{X_C}$ changes in order to satisfy (A10), i.e., the variations in the V's are determined from

$$Q_i = C_{0,i}(\vec{X}_C) + \sum_{j=1}^{N} C_{i,j}(\vec{X}_C) V_j(\vec{X}_C)$$
$$(i = 1,...,N). \quad (A12)$$

The second qualification is that there be no energy losses (stored energy converted into heat) when the selected conductor is displaced. There may be some free charge imbedded in the dielectric in the immediate vicinity of the selected conductor, but the conductor is not permitted to come into direct contact with any free charge during the displacement, because this charge would be irreversibly absorbed by the conductor. We must therefore imagine a thin layer of space which surrounds the selected conductor and is devoid of free charge. The mathematical significance of this statement is that sufficiently small changes in $\mathbf{X_C}$ from the actual conductor location do not change the right side of (A6b). Therefore, the gradient of (A6b), evaluated at the actual conductor location, is calculated by treating the right side as a constant, and the result is

$$\sum_{i=1}^{N} \vec{D}_{0,i} = 0 \quad (A13)$$

where the D's are defined by

$$\vec{D}_{i,j} \equiv \vec{\nabla}_C C_{i,j}(\vec{X}_C) \quad (\textit{all allowed } i, j). \quad (A14)$$

Subject to the qualifications (A12) and (A13), the force is calculated from (A11). Substituting (A9) into (A11) and taking the gradient gives

$$\vec{F} = -\frac{1}{2}\vec{D}_{0,0} - \frac{1}{2}\sum_{i,j=1}^{N} \vec{D}_{i,j} V_i V_j - \sum_{i=1}^{N} V_i \left[\sum_{j=1}^{N} C_{i,j} \vec{\nabla}_C V_j \right]. \quad (A15)$$

This equation is more convenient when written without gradients of the V's. For this purpose, we take the gradient of (A12) to get

$$\sum_{j=1}^{N} C_{i,j} \vec{\nabla}_C V_j = -\vec{D}_{0,i} - \sum_{j=1}^{N} \vec{D}_{i,j} V_j. \quad (i = 1,...N)$$

Using this equation to substitute for the bracket in (A15) gives

$$\vec{F} = \frac{1}{2}\sum_{i,j=1}^{N} \vec{D}_{i,j} V_i V_j + \sum_{i=1}^{N} \vec{D}_{0,i} V_i - \frac{1}{2}\vec{D}_{0,0}. \quad (A16)$$

It is possible to use constraints between the D's to write (A16) so that it contains fewer terms. One constraint is (A13). Other constraints are obtained from (A14) combined with (A6a) and (A6c), which gives

$$\vec{D}_{i,j} = \vec{D}_{j,i} \quad (i, j = 1,...,N) \quad (A17a)$$

$$\sum_{j=1}^{N} \vec{D}_{i,j} = 0 \quad (i = 1,...,N). \quad (A17b)$$

By using (A13) and (A17), it is possible to re-arrange (A16) into

$$\bar{F} = -\frac{1}{2}\sum_{i=1}^{N-1}\sum_{j=i+1}^{N}\bar{D}_{i,j}(V_i - V_j)^2 + \sum_{i=1}^{N}\bar{D}_{0,i}(V_i - V_M) - \frac{1}{2}\bar{D}_{0,0} \quad (A18)$$

where V_M is an arbitrary potential. It may be convenient (but not required) to let V_M be the potential of the selected conductor.

A5. *An Example*

The example considered is the problem relevant to the main text, shown in Figs.2 and 3. We will calculate the horizontal force that a single cell shown in Fig.3 exerts on the ME.

A region having a closed boundary can be constructed without including boundary surfaces at remote locations by including some artificial reflective boundaries. The force that will be calculated is the force for a hypothetical arrangement having such reflective boundaries. In order for the force for this hypothetical arrangement to approximate the force for the actual arrangement, it is necessary that the two arrangements have approximately the same electric field patterns. This requires that the artificial reflective boundaries be approximately tangent to the electric field lines in the actual arrangement. The electric field pattern relevant for this consideration is the one produced when the conductors are at the same potentials that produce the force to be calculated. The three upper electrodes will all be at different potentials, so, neglecting fringing near the top of these electrodes, the electric field near the top of and between the upper electrodes is approximately horizontal, as suggested in Fig.3. We also assume that the electric field, below and near the horizontal center of the two outer upper electrodes, is approximately vertical. We can therefore include artificial reflective boundaries shown as the dashed lines in Fig.A2. This produces a closed boundary, as required by the theory (the problem is approximated as two-dimensional, so a closed curve in the plane of the page qualifies as a closed boundary surface).

The upper fixed electrodes are S_1 and S_2, the ME is S_3, and the lower conductive plane is S_4. The dimensions h_e, h_g, h_d, A_1, A_2, and A_3 are defined in Fig.A2. A length L is the depth into the page. The quantities A_1 and A_2 are somewhat arbitrary (the horizontal locations of the artificial vertical reflective boundaries are somewhat arbitrary), so it is fortunate that they will not appear in the final equations.

We are required to calculate variations in several quantities produced by variations in the ME location, so it is necessary to introduce a variable coordinate describing the ME location. Only one coordinate, describing the horizontal position, is needed to calculate the horizontal force. It is convenient to let X_C refer to the displacement from the center position. Let W be the vertical air gap width on either side of the ME when the ME is centered, so W and X_C are as shown in Fig.A2. Note that X_C is positive when the ME is displaced to the right in the figure. Horizontal components of vectors will refer to this direction, so the horizontal component of the gradient in (A14) is $\partial/\partial X_C$.

We start with the elementary potential ϕ_0. Boundary conditions and a sketch of the electric field pattern produced by this potential are shown in Fig.A3. The figure shows a positive charge layer inside the dielectric, but the analysis applies to an arbitrary one-dimensional charge versus depth profile. The vertical air gap width is smaller than the widths of the upper electrodes, so the electric field is approximately uniform below the lower electrodes. Let y be the vertical coordinate with y=0 at the lower electrode, so $y=h_T$ at the bottom of the upper electrodes, where $h_T \equiv h_d + h_g$. For y between 0 and h_T, (A1) reduces to

$$\frac{d}{dy}\left[\varepsilon\frac{d\phi_0}{dy}\right] = -\rho \quad for \quad 0 < y < h_T$$

$$\phi_0 = 0 \quad at\ y = 0\ and\ at\ y = h_T$$

with solution

$$\left[\int_0^{hT}\frac{1}{\varepsilon(y')}dy'\right]\phi_0(y) = \left[\int_0^{y}\frac{1}{\varepsilon(y')}dy'\right]\int_y^{hT}\left[\int_{y'}^{hT}\frac{1}{\varepsilon(y'')}dy''\right]\rho(y')dy' + \left[\int_y^{hT}\frac{1}{\varepsilon(y')}dy'\right]\int_0^{y}\left[\int_0^{y'}\frac{1}{\varepsilon(y'')}dy''\right]\rho(y')dy'$$

which can be verified by verifying that it satisfies the boundary value problem. Using the above equation, while noting that $\varepsilon=\varepsilon_0$ and $\rho=0$ above the dielectric gives

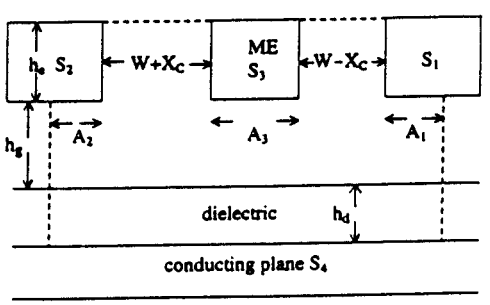

Fig.A2: Artificial reflective boundaries (dashed lines) produce a closed boundary for a simplified approximation. Geometric dimensions are also shown, except L which is into the page.

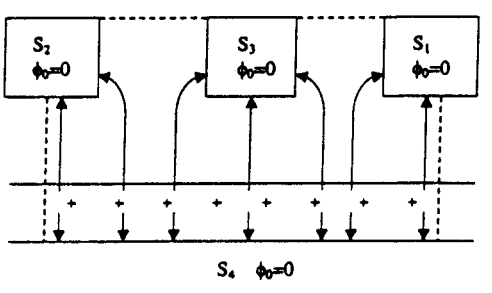

Fig.A3: Boundary conditions for ϕ_0, and a sketch of a few field lines.

$$\left[\varepsilon\frac{d\phi_0}{dy}\right]_{y=0} = \sigma$$

$$-\left[\frac{h_g}{\varepsilon_0}+\frac{h_d}{\varepsilon_{eff}}\right]^{-1}\int_0^{hd}\left[\int_0^{y'}\frac{1}{\varepsilon(y'')}dy''\right]\rho(y')dy'$$

$$\left[\varepsilon\frac{d\phi_0}{dy}\right]_{y=hT} =$$

$$-\left[\frac{h_g}{\varepsilon_0}+\frac{h_d}{\varepsilon_{eff}}\right]^{-1}\int_0^{hd}\left[\int_0^{y'}\frac{1}{\varepsilon(y'')}dy''\right]\rho(y')dy'$$

where the dielectric charge per unit area, σ, is defined by

$$\sigma \equiv \int_0^{hd}\rho(y)dy \qquad (A19)$$

and an effective dielectric constant, ε_{eff}, for a (possibly) inhomogeneous dielectric is defined by

$$\frac{h_d}{\varepsilon_{eff}} \equiv \int_0^{hd}\frac{1}{\varepsilon(y)}dy. \qquad (A20)$$

To shorten the notation, we define a weighted average or effective height, h_{eff}, for the dielectric charge distribution by

$$h_{eff} \equiv \frac{\varepsilon_{eff}}{\sigma}\int_0^{hd}\left[\int_0^{y}\frac{1}{\varepsilon(y')}dy'\right]\rho(y)dy. \qquad (A21)$$

If the dielectric is homogeneous and if the charge is confined to a thin layer, h_{eff} is the height of this layer above the lower electrode. Whether the dielectric is homogeneous or not, if the charge is confined to a thin layer at the top of the dielectric, $h_{eff}=h_d$. Substituting (A21) into the equations for the derivative of ϕ_0 gives

$$\left[\varepsilon\frac{d\phi_0}{dy}\right]_{y=0} = \sigma - \frac{h_{eff}\,\varepsilon_0}{h_g\,\varepsilon_{eff}+h_d\,\varepsilon_0}\sigma \qquad (A22a)$$

$$\left[\varepsilon\frac{d\phi_0}{dy}\right]_{y=ht} = -\frac{h_{eff}\,\varepsilon_0}{h_g\,\varepsilon_{eff}+h_d\,\varepsilon_0}\sigma. \qquad (A22b)$$

Although not needed to calculate the force, the main text has a need for ϕ_0 evaluated at the top of the dielectric. Evaluating the equation for ϕ_0 at $y=h_d$, while using (A19), (A20), and (A21) to simplify the notation, gives

$$\varphi_0(h_d) = \frac{h_{eff}\,h_g}{h_g\,\varepsilon_{eff}+h_d\,\varepsilon_0}\sigma. \qquad (A23)$$

The next step is to calculate the C's and D's having a zero subscript. The C's are only needed to calculate the D's, so we do not have to calculate $C_{0,0}$, because $D_{0,0}$ is already known. In the dielectric where ρ may differ from zero, ϕ_0 calculated above does not depend on X_C. Therefore, $C_{0,0}$ given by (A5a) does not depend on X_C, so (A14) produces our first result, which is

$$D_{0,0} = 0. \qquad (A24)$$

To calculate $C_{0,1},\ldots, C_{0,4}$, we note from (A5b) that these are the electric field fluxes through each of the four electrodes. Although the electric field associated with ϕ_0 was approximated as uniform in the dielectric and horizontal air gap, there is still fringing in the vertical air gaps, which bends the field lines entering these gaps so that the field lines terminate on electrodes. Electric field lines entering a vertical gap and terminating on an electrode contribute to the flux through that electrode. Note that the flux through the right side of S_2 (Fig.A3) plus the flux through the left side of S_3 equals the flux entering the air gap between S_2 and S_3. The two former fluxes are very nearly equal, so the flux through the right side of S_2 is one-half the flux entering the vertical air gap. The total flux through S_2 is the flux through a horizontal planar section at the bottom of the upper electrodes and having a width of A_2 plus one-half the air gap width. This gives

$$C_{0,2} = L\left[A_2+\frac{1}{2}(W+X_C)\right]\left[\varepsilon\frac{d\phi_0}{dy}\right]_{y=ht} \qquad (A25)$$

and using (A22b) gives

$$C_{0,2} = -L\left[A_2+\frac{1}{2}(W+X_C)\right]\frac{h_{eff}\,\varepsilon_0\,\sigma}{h_g\,\varepsilon_{eff}+h_d\,\varepsilon_0}. \qquad (A26a)$$

Similar considerations for S_1 give

$$C_{0,1} = -L\left[A_1+\frac{1}{2}(W-X_C)\right]\frac{h_{eff}\,\varepsilon_0\,\sigma}{h_g\,\varepsilon_{eff}+h_d\,\varepsilon_0}. \qquad (A26b)$$

The flux through S_4 is obviously given by

$$C_{0,4} = -[A_1+A_2+A_3+2W]\left[\varepsilon\frac{d\phi_0}{dy}\right]_{y=0} \qquad (A26c)$$

where the bracket on the right is given by (A22a). Because of the constraint (A6b), we are not required to calculate $C_{0,3}$, although we can as a matter of curiosity. Calculating $C_{0,3}$ using the same methods used to calculate $C_{0,1}$ and $C_{0,2}$ verifies that (A6b) is satisfied. The D's are calculated from

$$D_{i,j} = \frac{dC_{i,j}}{dX_C} \qquad (A27)$$

and using (A26) gives

$$D_{0,1} = \frac{1}{2}\frac{L h_{eff}\,\varepsilon_0\,\sigma}{h_g\,\varepsilon_{eff}+h_d\,\varepsilon_0} \qquad (A28a)$$

$$D_{0,2} = -\frac{1}{2}\frac{L h_{eff}\,\varepsilon_0\,\sigma}{h_g\,\varepsilon_{eff}+h_d\,\varepsilon_0} \qquad (A28b)$$

$$D_{0,4} = 0. \qquad (A28c)$$

We next consider ϕ_4 because the analysis is very similar to that for ϕ_0. Boundary conditions and a sketch of the electric field pattern produced by this potential are shown in Fig.A4. As with ϕ_0, we neglect fringing below the upper electrodes, so we calculate ϕ_4 in this region from the one-dimensional problem given by

$$\frac{d}{dy}\left[\varepsilon\frac{d\phi_4}{dy}\right]=0 \quad for \quad 0<y<h_T$$

$$\phi_4 = 1\ at\ y=0\ and\ \phi_4 = 0\ at\ y=h_T$$

with solution

$$\phi_4 = 1-\left[\frac{h_d}{\varepsilon_{eff}}+\frac{h_g}{\varepsilon_0}\right]^{-1}\int_0^y \frac{1}{\varepsilon(y')}dy'$$

so that

$$\varepsilon\frac{d\phi_4}{dy} = -\frac{\varepsilon_{eff}\,\varepsilon_0}{h_g\,\varepsilon_{eff}+h_d\,\varepsilon_0}$$

$$for \quad 0<y<h_T. \quad (A29)$$

The calculations of $C_{4,i}$ ($=C_{i,4}$) and $D_{4,i}$ ($=D_{i,4}$) are similar to those for $C_{0,i}$ and $D_{0,i}$. The results are

$$C_{1,4} = -L\left[A_1+\frac{1}{2}(W-X_C)\right]\frac{\varepsilon_{eff}\,\varepsilon_0}{h_g\,\varepsilon_{eff}+h_d\,\varepsilon_0}$$

$$C_{2,4} = -L\left[A_2+\frac{1}{2}(W+X_C)\right]\frac{\varepsilon_{eff}\,\varepsilon_0}{h_g\,\varepsilon_{eff}+h_d\,\varepsilon_0}$$

$$C_{3,4} = -L[A_3+W]\frac{\varepsilon_{eff}\,\varepsilon_0}{h_g\,\varepsilon_{eff}+h_d\,\varepsilon_0}$$

$$D_{1,4} = \frac{1}{2}\frac{L\varepsilon_{eff}\,\varepsilon_0}{h_g\,\varepsilon_{eff}+h_d\,\varepsilon_0} \quad (A30a)$$

$$D_{2,4} = -\frac{1}{2}\frac{L\varepsilon_{eff}\,\varepsilon_0}{h_g\,\varepsilon_{eff}+h_d\,\varepsilon_0} \quad (A30b)$$

$$D_{3,4} = 0. \quad (A30c)$$

We next consider ϕ_1. Boundary conditions and a sketch of the electric field pattern produced by this potential are shown in Fig.A5. Note that $C_{1,4}$ was already calculated, so we need ϕ_1 only to calculate $C_{1,2}$ and $C_{1,3}$. The quantity $C_{1,3}$ is determined by the electric field lines connecting S_1 to S_3. The dimension h_e in Fig.A2 is much larger than the air gap W, suggesting that a no-fringing approximation for ϕ_1 in the air gap may produce an adequate estimate of $C_{1,3}$. Note that there is a distinction between $C_{1,3}$ and the C's previously calculated in terms of required accuracy. To discuss this, we define some terminology. The force on the ME produced by specified electrode potentials but in the absence of a dielectric charge will be called the nominal force. The change in the force on the ME produced by adding a dielectric charge, while maintaining the electrode potentials, will be called the excess force. The electric field fringing in Fig.A3 (the connection of field lines to the electrodes via field line bending in the vertical air gaps) are needed to obtain an excess horizontal force. Therefore, it is essential that calculations include field lines entering the air gaps if we want to predict a nonzero excess horizontal force. Similarly, it is essential that calculations include field lines entering the air gap in Fig.A4 if we want to predict the influence that S_4 has on the nominal horizontal force. In contrast, calculations need not include fringing to predict a nominal horizontal force between S_1 and S_3, fringing is only needed to make the calculations accurate to many digits. Assuming that our accuracy requirements will tolerate a moderate fractional or percent error in the nominal force (certainly true if our only interest is in the excess force), a no-fringing approximation for ϕ_1 is adequate for calculating $C_{1,2}$ and $C_{1,3}$. The results are

$$C_{1,2} = 0$$

$$C_{1,3} = -\frac{Lh_e\,\varepsilon_0}{W-X_C}.$$

Similar considerations for ϕ_2 give

$$C_{2,3} = -\frac{Lh_e\,\varepsilon_0}{W+X_C}$$

so the D's are given by

$$D_{1,2} = 0 \quad (A31a)$$

$$D_{1,3} = -\frac{Lh_e\,\varepsilon_0}{(W-X_C)^2} \quad (A31b)$$

$$D_{2,3} = \frac{Lh_e\,\varepsilon_0}{(W+X_C)^2}. \quad (A31c)$$

Constraints were used to eliminate redundant D's, that can be calculated from others, from (A18). Taking V_M to be V_3, the only D's appearing in (A18) are those calculated from (A24), (A28), (A30), and (A31). Substituting for these D's in (A18) while using $V_4=V_3$ gives

$$F = F_{nom} + F_{excess} \quad (A32a)$$

where F_{nom} is the nominal force given by

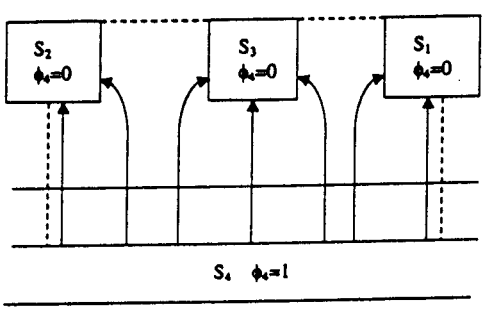

Fig.A4: Boundary conditions for ϕ_4, and a sketch of a few field lines.

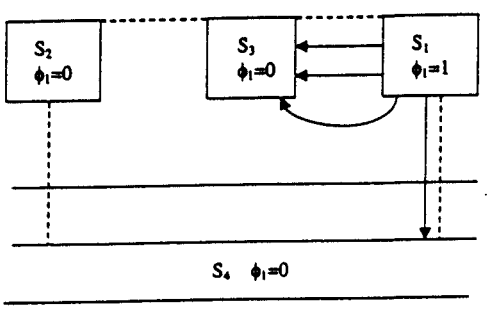

Fig.A5: Boundary conditions for ϕ_1, and a sketch of a few field lines.

$$F_{nom} = \frac{1}{2} L h_e \varepsilon_0 \left[\frac{(V_1 - V_3)^2}{(W - X_C)^2} - \frac{(V_2 - V_3)^2}{(W + X_C)^2} \right]$$
$$- \frac{1}{4} \frac{L \varepsilon_{eff} \varepsilon_0}{h_g \varepsilon_{eff} + h_d \varepsilon_0} \left[(V_1 - V_3)^2 - (V_2 - V_3)^2 \right] \quad (A32b)$$

and F_{excess} is the excess force given by

$$F_{excess} = \frac{1}{2} \frac{L h_{eff} \varepsilon_0 \sigma}{h_g \varepsilon_{eff} + h_d \varepsilon_0} (V_1 - V_2). \quad (A32c)$$